

A New Analytical Redesign of a Double-Curvature Reflector Antenna Using Invasive Weed Optimization (IWO) Algorithm

Ali Vedaee, Gholamreza Askari*, Hamid Mirmohammad Sadeghi, and Mehdi Fadaei

Abstract—This paper presents an efficient method to redesign a horn-fed, double-curvature reflector antenna. It helps reconstruct or repair the reflector according to a correct reference or analyze its radiation characteristics through full-wave electromagnetic simulations. The proposed method mainly consists of five stages. At first, it is necessary to obtain initial data in the form of three-dimensional coordinates of a sufficient number of points sampled from the reflector's different surface areas, especially from its central section curve and its peripheral contour. Then, the best-fitting surface to the sampled points is found using geometrical-optics (GO)-based formulations in an invasive weed optimization (IWO) algorithm. The GO relations extend the reflector laterally using elevation angle, horizontal, or focal point strips. As these are intrinsic formulations for designing doubly-curved reflectors, the fitted surface can resolve the possible defects in the reference reflector's geometry or inaccuracies in the sampled information partly. For this purpose, the reflector's central section curve is estimated by fitting a fifth-degree polynomial curve to the data sampled from it. Also, two kinds of errors, which are based on Euclidean distances, define the optimization algorithm cost function for more reliable surface fitting. In the third stage, the fitted surface's peripheral contour is adjusted to match the outline of the reference reflector using the points sampled from this section. In stage four, the redesigned reflector in the form of a point cloud is converted to a .stl file format for further simulation in a full-wave electromagnetic software. Finally, the similarity between the redesigned and reference reflectors' radiation patterns is examined using a radiation-based cost function in an iterative process, and the previously devised four stages repeat until appropriate results are obtained. In particular, an already designed and fabricated UHF band, doubly-curved reflector antenna, capable of generating a cosecant-squared radiation pattern in the elevation plane and narrow in the azimuth, is redesigned using 99 points sampled from it. It is found that horizontal strips can best fit the reflector with the small normalized error about 3 mm at the end of the IWO algorithm, indicating a nearly perfect geometrical similarity between the redesigned and reference reflectors. For further verification of the suggested method, the redesigned reflector's radiation pattern is simulated in CST simulation software, and the results are compared with the measured radiation pattern of the fabricated reflector and the simulated radiation pattern of the antenna's initial CAD model in the azimuth and elevation planes. Specifically for the redesigned antenna, the amounts of HPBW and sidelobe level in the azimuth plane are about 2.6° and 29.85 dB, respectively. Also, the amounts of gain, HPBW, and predefined parameters of α and β in the elevation plane are 28.25 dB, 13.5° , 5.07 dB, and 11.7° , respectively. All of the measured and simulated results are in good correspondence with each other, suggesting that the proposed method is a secure solution for redesigning double-curvature reflector antennas precisely and efficiently.

1. INTRODUCTION

In some microwave radar applications, it is necessary to receive a nearly constant power from a target moving at the same vertical distance from the horizontal plane. This is achievable by an antenna with a

Received 17 March 2021, Accepted 3 August 2021, Scheduled 13 August 2021

* Corresponding author: Gholamreza Askari (askarigh@iut.ac.ir).

The authors are with the Research Institute for Information and Communication Technology (ICTI), Isfahan University of Technology (IUT), Isfahan 84156-83111, Iran.

narrow beam in the azimuth plane and a cosecant-squared-like radiation pattern in the elevation [1–3]. If it is assumed that \mathbf{r} is the vector from this antenna to the target point, θ is the angle between the horizontal plane and vector \mathbf{r} , and h is the vertical distance between the antenna and the target point. The relationship between these parameters can be described as:

$$|\mathbf{r}| = h \times \csc \theta \quad (1)$$

On the other hand, the radiation power of an antenna in a given direction θ is proportional to $1/|\mathbf{r}|^2$ in the far-field region [4]. Therefore, to receive a nearly constant reflected energy from a target, moving at the same vertical distance, the antenna's gain pattern must be proportional to $(\csc \theta)^2$ in the elevation plane. Hence, these are frequently named cosecant-squared radiation pattern antennas. The said proportionality must be held from a minimum angle of $\sin^{-1} h/|\mathbf{r}|_{\max}$ to the maximum elevation angle for which the coverage is required [3].

Cosecant-squared radiation pattern antennas have been implemented in diverse configurations, such as doubly-curved reflectors [5–9], reflectarrays [10–13], and pillboxes [14]. Among them, double-curvature reflectors are widely used in navigational systems due to their outstanding functionalities.

The logical evolution of these antennas may be originated in 1964 when Silver [3] determined optical conditions for a double-curvature reflector using Chu's method [2] to obtain its central-section curve equation [1]. In 1948, Dunbar reported a work, based on energy conservation and simple GO laws on doubly-curved reflector antennas [1]. His suggested method determines the reflector's central section curve equation, considering its focal point relative location and the antenna's primary and secondary radiation patterns. A finely designed stack of parabolic strips passing through elevation angle planes extends the reflector surface in the transverse direction. In 1971, Bruner proposed a method similar to the one presented in [1]; however, in this case, transverse strips are either parabolas, located in elevation angle planes, or ellipses located in horizontal or focal point planes, offering different radiation and geometrical characteristics [15].

These works are in the context of doubly-curved reflector antennas synthesis; however, sometimes, it is necessary to redesign a doubly-curved reflector antenna for reconstructing or repairing it according to a correct reference or analyzing its radiation pattern through full-wave electromagnetic simulations. Redesigning a doubly-curved reflector for reconstruction purposes obviates the need for designing its feeding antenna or transceiver apparatus again, which may be a challenging and time-consuming task. This necessity may be highlighted when a country imports a navigational system with a doubly-curved reflector, without any access to the antenna's design specifications. In this situation, redesigning the imported reflector is an excellent solution for producing the system in its territory for self-sufficiency. To the best of the authors' knowledge, there has been no reported work on redesigning double-curvature reflector antennas in the literature.

One way to redesign a double-curvature reflector is to sample 3D coordinates of a sufficient number of points from it and find the best-fitting surface to the sampled points using the available surface fitting approaches. These general approaches include using polynomial functions, tensor product and blending methods, or surface splines [16]. These methods can yield a texture that fits the sampled points accurately; however, if there are slight deformations or asymmetries in the reflector structure or inaccuracies in the initial data, these distortions will affect the resulting surface considerably, because these approaches do not have any insight into the electromagnetic functionality of the reflector structure.

In contrast to the general surface fitting approaches, the suggested method employs intrinsic, geometrical-optics (GO)-based formulations for surface fitting. These formulations form the double-curvature surface using elevation angle, horizontal, or focal point strips [1, 15] which are generally used in the initial design of these reflectors. Therefore, the fitting surface in this method is the most similar one to the ideal surface designed initially and is less vulnerable to the possible defects in the reflector geometry or inaccuracies in the sampled information, as compared to using the general surface fitting approaches. It should be noted that the surface fitting process is done using an invasive weed optimization (IWO) algorithm, which is a population-based evolutionary method initially reported in [17] and inspired by weed colonies' behavior [18].

Particularly, the method of redesigning a UHF band, horn fed, double-curvature reflector antenna with a cosecant-squared-like radiation pattern in the elevation plane and narrow in the azimuth is presented in this paper. The design procedure for such a reflector antenna is as follows. First, its primary and secondary radiation patterns in the elevation plane are determined. The primary radiation

pattern refers to the horn antenna's pattern, and the secondary radiation pattern is the pattern of the whole reflector antenna system. Then, the reflector's central section curve is specified using these two patterns, conservation of energy, and simple geometrical-optics principles. Based on this curve definition and applying geometrical optics for collimating the antenna's radiation pattern in the transverse plane, its surface can be established using transverse strips. After some optimizations, the position and orientation of the horn are adjusted such that its aperture is almost coincident with the reflector's focal point, and the desired radiation pattern is generated in the azimuth and elevation planes. Its final CAD model is processed mechanically, and the reflector is fabricated using a net of wires which reduces its weight and resistance to the wind considerably. Figure 1 illustrates the reflector initial CAD model. The simulated radiation pattern of this model and the measured radiation pattern of the fabricated reflector are used as a reference for the redesign approach quality examination in Section 3.

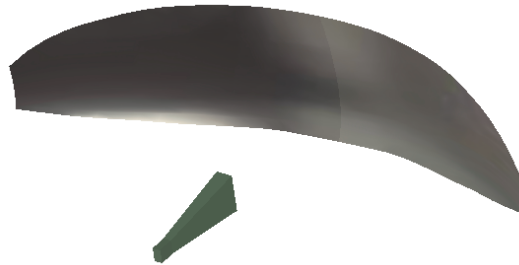


Figure 1. Initial CAD model of the designed and fabricated horn-fed reflector antenna with cosecant-squared-like radiation pattern in the elevation plane and narrow in the azimuth.

The paper is organized as follows. Section 2 explains the necessary information for redesigning a double-curvature reflector, the method of fitting a surface to it using the GO-based formulations, and the employed IWO algorithm. Besides, adjusting the surface's peripheral contour, converting the redesigned surface to a suitable CAD file format, and optimizing the redesigned surface according to its radiation pattern characteristics are discussed in this section. Section 3 examines the proposed method efficiency by comparing the simulated radiation patterns of the redesigned reflector and the measured radiation pattern of the fabricated reflector or the simulated radiation pattern of the reflector's initial CAD model. Conclusions are drawn in Section 4.

2. REDESIGN PROCEDURE

2.1. Sampling the Initial Information

For redesigning a double-curvature reflector antenna using the conventional GO-based formulations [1, 15], the following items must be known:

- a1.1- Reflector's central section curve shape
- a1.2- Reflector's peripheral contour shape
- a1.3- Reflector's focal point optimum location
- a1.4- Optimum type of strips to extend the reflector in the transverse direction
- a1.5- Optimum horizontal plane direction for redesigning the reflector using horizontal strips

From the above information, only the reflector's central section curve and its peripheral contour can be estimated using physical measurements, and there is no exact information about the other three items (a1.3 to a1.5). The reflector's central section curve is the cross-section of a double-curvature reflector with its symmetry plane.

For recompensing the information shortage, the proposed solution is to exploit another information, existing in the reflector surface, to derive the required data. Thus, the recommended necessary information for redesigning a doubly-curved reflector is three-dimensional coordinates of a sufficient number of points sampled from the following reflector parts:

- a2.1- Reflector's central section curve
- a2.2- Reflector's peripheral contour
- a2.3- General areas of the reflector surface

The aim is to use this information (a2.1 to a2.3) in an efficient optimization algorithm to derive the required data (a1.1 to a1.5) for redesigning the reflector. In this process, the best-fitting surface to the sampled points is found using geometrical-optics-based formulations, as explained in the next section.

Two different methods are suggested to obtain 3D coordinates of the sampled points. The first method which is employed here is based on the fact that if the distances between an arbitrary point P in space and at least four non-coplanar reference points with known 3D coordinates are found, the 3D coordinates of point P can be determined uniquely. Implementation of this method is shown in Figure 2(a) with a wooden board installed on the aperture of the reflector's feeding horn antenna. Points M_1 to M_4 are the four reference points with known 3D coordinates in the XYZ Cartesian coordinate system defined on the board (inset picture). Z -axis is assumed to be normal to the board surface. Four other reference points are located on the reflector surface with their 3D coordinates defined in the XYZ coordinate system. The distances between an arbitrary sampled point P and these eight reference points are used to estimate its 3D coordinates. Figure 2(b) shows the sampled points marked with the paper targets on the reflector to extract their 3D coordinates. The second proposed approach

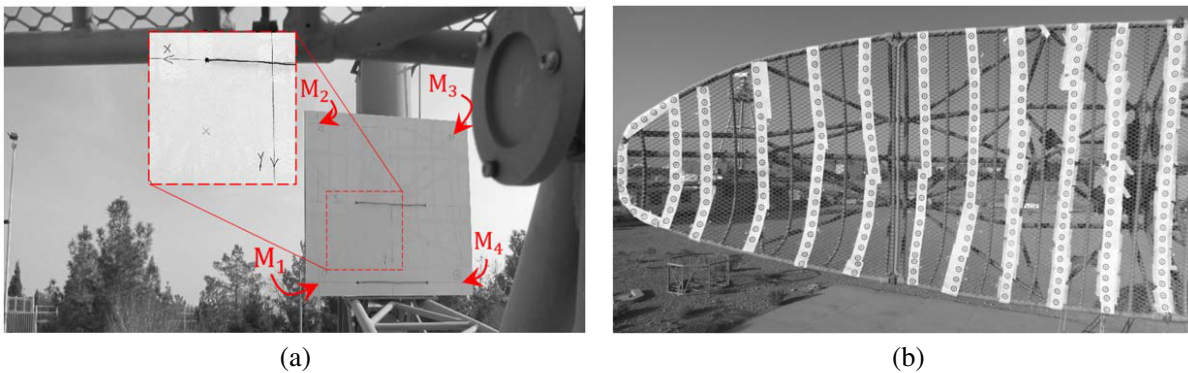


Figure 2. (a) The wooden board installed on the aperture of the reflector's feeding horn antenna. Four marked points M_1 to M_4 are shown with the tips of the arrows. Also, the marked XYZ Cartesian coordinate system is shown in the inset picture for better visibility. Z -axis is considered to be normal to the board surface. (b) The cosecant-squared radiation pattern reflector antenna and the sampled points, marked with the attached paper targets.

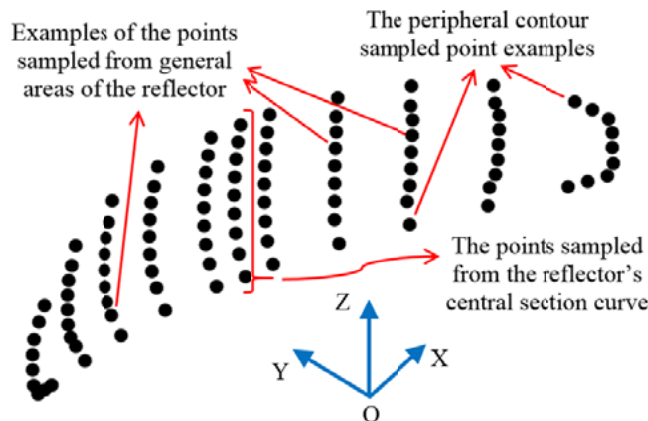


Figure 3. The points sampled from the reflector's central section curve, its peripheral contour, and its general surface areas.

uses the photogrammetry method for finding the sampled points' 3D coordinates. Photogrammetry is a high-speed, accurate and comfortable method that can be used for modeling and measuring small to large objects and areas effectively.

The use of these two techniques for redesigning double-curvature reflector antennas will be presented in a separate article by the authors for future publication. The points can also be sampled from the initial CAD model of the reflector to simplify the redesign process.

Figure 3 shows the 99 points sampled from the UHF band reflector's central section curve, its peripheral contour, and its general surface areas. It is better to sample the points from different reflector areas uniformly for taking into account all of the reflector's geometrical behavior nearly the same.

2.2. Finding the Best-Fitting Surface to the Sampled Points Using GO Formulations

According to the proposed method for optimum redesigning the reflector using GO-based formulations, the sampled points must be defined appropriately in a Cartesian coordinate system as illustrated approximately in Figure 3. In this definition, the coordinate system's origin O determines the focal point for redesigning the reflector. Its YZ plane describes the reflector's symmetry plane, and the XY plane is parallel to the horizontal direction for redesigning using horizontal strips. This proper definition of the sampled points in the Cartesian coordinate system is attained using an invasive weed optimization algorithm.

For this purpose, an initial definition of the sampled points in the XYZ coordinate system is illustrated in Figure 4, which is used as a reference arrangement in the optimization algorithm. In this arrangement, the coordinate system's origin coincides with the uppermost point sampled from the reflector's central section curve, and its axes are oriented similar to the XYZ coordinate system, shown in Figure 3. The optimization goal is to find the best location and orientation of the sampled points collection, for finding the best fitting surface to it using elevation angle, horizontal, or focal point strips. For this purpose, the parameters $\alpha_x, \alpha_y, \alpha_z, t_x, t_y,$ and t_z are defined as the optimization parameters and are used to rotate and then translate the set of sampled points to any arbitrary orientation and position in space as described in Table 1. As can be seen, α_x is an optimization parameter used for redesigning the reflector with horizontal strips only, because solely redesigning the reflector using this

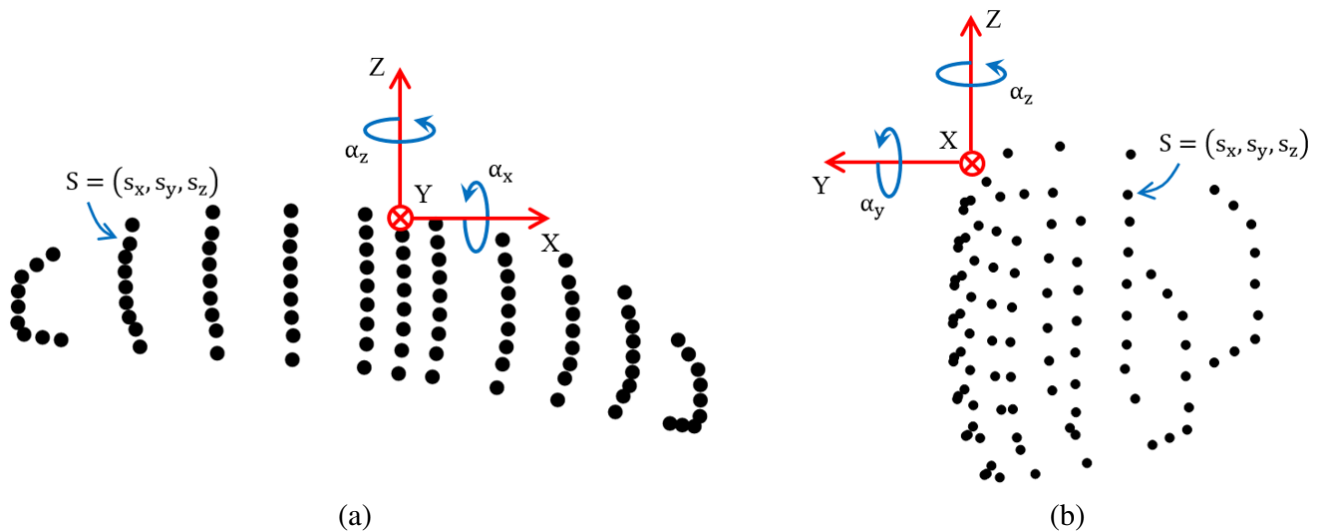


Figure 4. Initial definition of the points sampled from the reflector surface in the XYZ Cartesian coordinate system in the optimization operation. (a) Observation point along Y -axis. (b) Observation point along X -axis. In this definition, the Cartesian coordinate system's origin is located on the uppermost point sampled from the reflector's central section curve, its X -axis is nearly transversely oriented, and its Z -axis is almost orthogonal to the horizontal plane.

Table 1. Description of the optimization parameters for redesigning a double-curvature reflector using the suggested method.

| Optimization parameter | Description | For redesigning the reflector using |
|------------------------|--|---|
| α_x | Sampled points group rotation angle around the X -axis | Horizontal strips |
| α_y | Sampled points group rotation angle around the Y -axis | Elevation angle, horizontal or focal point strips |
| α_z | Sampled points group rotation angle around the Z -axis | Elevation angle, horizontal or focal point strips |
| t_x | Sampled points group translation along the X -axis | Elevation angle, horizontal or focal point strips |
| t_y | Sampled points group translation along the Y -axis | Elevation angle, horizontal or focal point strips |
| t_z | Sampled points group translation along the Z -axis | Elevation angle, horizontal or focal point strips |

type of strip depends on the horizontal plane direction definition. The rotation angles are defined to be positive for a rotation that is counterclockwise when viewed by an observer looking along the rotation axis towards the origin.

Accordingly, for redesigning the reflector using elevation angle, horizontal, or focal point strips, the optimization parameters can be defined in the form of vectors as described in Eqs. (2)–(4), respectively:

$$\mathbf{V}_E = (\alpha_y, \alpha_z, t_x, t_y, t_z) \quad (2)$$

$$\mathbf{V}_H = (\alpha_x, \alpha_y, \alpha_z, t_x, t_y, t_z) \quad (3)$$

$$\mathbf{V}_F = \mathbf{V}_E \quad (4)$$

By defining the optimization parameters and selecting the type of strips for finding the best-fitting surface to the sampled points, the first step in the IWO algorithm is to generate the first colony of weeds as a set of optimization vectors with random distribution in the search space. In this manner, each optimization vector defines a unique location and orientation of the sampled points in space.

For each of the optimization vectors in the set (colony), the sampled points collection is rotated around X , Y , and Z coordinate axes with the amounts of α_x (if necessary), α_y , and α_z , respectively. Therefore, the relation between three-dimensional coordinates of an arbitrary sampled point S (Figure 4) before rotation (s_x, s_y, s_z) and after that $(s_{x,r}, s_{y,r}, s_{z,r})$ can be described as:

$$\begin{bmatrix} s_{x,r} \\ s_{y,r} \\ s_{z,r} \end{bmatrix} = R_z(\alpha_z) \times R_y(\alpha_y) \times R_x(\alpha_x) \times \begin{bmatrix} s_x \\ s_y \\ s_z \end{bmatrix} \quad (5)$$

where $R_x(\alpha_x)$, $R_y(\alpha_y)$, and $R_z(\alpha_z)$ are the coordinate system rotation matrices around the X , Y , and Z axes respectively as defined in Eqs. (6) to (8) [19]:

$$R_x(\alpha_x) = \begin{bmatrix} 1 & 0 & 0 \\ 0 & \cos \alpha_x & -\sin \alpha_x \\ 0 & \sin \alpha_x & \cos \alpha_x \end{bmatrix} \quad (6)$$

$$R_y(\alpha_y) = \begin{bmatrix} \cos \alpha_y & 0 & \sin \alpha_y \\ 0 & 1 & 0 \\ -\sin \alpha_y & 0 & \cos \alpha_y \end{bmatrix} \quad (7)$$

$$R_z(\alpha_z) = \begin{bmatrix} \cos \alpha_z & -\sin \alpha_z & 0 \\ \sin \alpha_z & \cos \alpha_z & 0 \\ 0 & 0 & 1 \end{bmatrix} \quad (8)$$

According to Euler’s rotation theorem, any arbitrary rotation of the sampled points can be realized using a combination of these three rotation matrices. Next to the rotation, the sampled points group is translated along the X , Y , and Z coordinate axes with the amounts of t_x , t_y , and t_z , respectively. Therefore, three-dimensional coordinates of an arbitrary sampled point S after a sequence of rotations and translations $(s_{x,rt}, s_{y,rt}, s_{z,rt})$ can be described by Eq. (9):

$$\begin{bmatrix} s_{x,rt} \\ s_{y,rt} \\ s_{z,rt} \end{bmatrix} = \begin{bmatrix} s_{x,r} \\ s_{y,r} \\ s_{z,r} \end{bmatrix} + \begin{bmatrix} t_x \\ t_y \\ t_z \end{bmatrix} \tag{9}$$

where $(s_{x,r}, s_{y,r}, s_{z,r})$ is given in Eq. (5). In this way, an arbitrary definition of the sampled points in 3D space can be obtained using the sequence of rotation and translation as specified above. Figure 5 shows the sampled points in the XYZ Cartesian coordinate system after an arbitrary sequence of rotation around and translation along the coordinate axes.

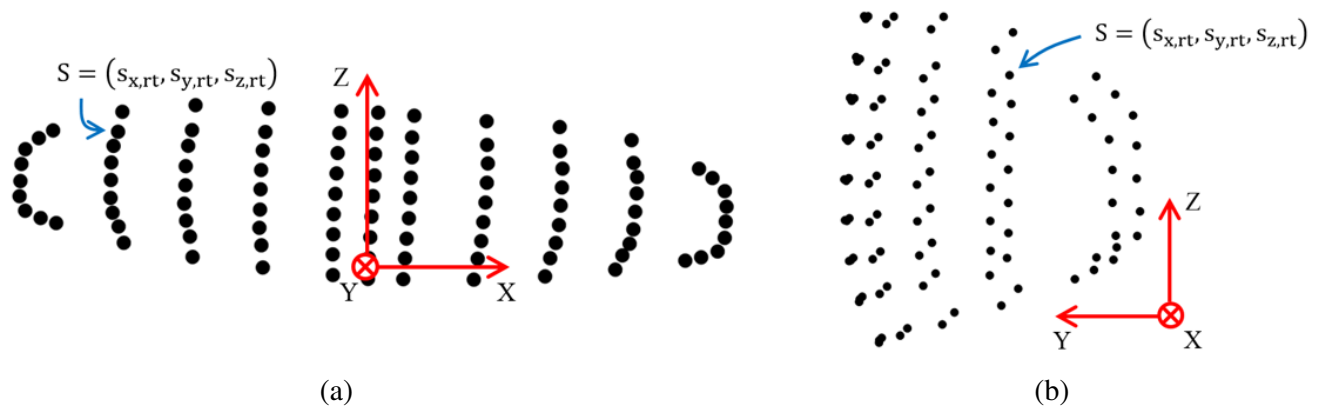


Figure 5. The points sampled from the reflector surface after rotating them around and translating along the XYZ Cartesian coordinate axes according to an optimization parameter vector. (a) Observation point along Y -axis. (b) Observation point along X -axis.

Following the sampled points translation, the reflector’s central section curve is estimated using the projection of the points sampled from this curve on the YZ plane. As can be seen in Figure 3, there are 9 points sampled from this curve on the reflector. So it seems reasonable to estimate this curve using curve fitting with a fifth-degree polynomial. The estimated curve is defined in discretized form for further analysis simplification.

Figure 6(a) illustrates the estimated reflector’s central section curve with the feeding horn located on focal point O . In this figure, parameter P defines the distance between focal point O and incident point I . The incident ray is shown with a solid arrow, while the reflected beam is shown with a dashed arrow. Also, the definition of the planes passing through the elevation angle, horizontal or focal point directions and their relation with the angles θ and ϕ are presented in Figure 6(a). The relation between the angles θ , ϕ in discretized form can be defined using Eq. (10):

$$\beta = \tan^{-1} \left(2 \frac{\Delta p}{p \Delta \phi} \right) \tag{10}$$

where:

$$\beta = \theta + \phi \tag{11}$$

By knowing the relation between the θ and ϕ , it is possible to extend the fitting surface in transverse direction for different ϕ angles using the stack of elevation angle, horizontal or focal point strips as specified in Eqs. (12) to (14), respectively:

$$\eta^2 = 2P\zeta_E [1 + \cos \beta] \tag{12}$$

$$\frac{\eta^2}{P^2 [(\cos \phi + \cos \theta) / \sin \theta]^2} + \frac{[\zeta_H - P (\cos \phi + \cos \theta) / (\sin \theta)^2]^2}{P^2 [(\cos \phi + \cos \theta) / (\sin \theta)^2]^2} = 1 \quad (13)$$

$$\frac{\eta^2}{P^2 [\sin \beta / (1 - \cos \beta)]^2} + \frac{[\zeta_F - P / (1 - \cos \beta)]^2}{P^2 [1 / (1 - \cos \beta)]^2} = 1 \quad (14)$$

where η is the abscissa variable in the transverse direction of the reflector, and ζ_E , ζ_H , and ζ_F are the ordinate variables in the planes passing through the elevation, horizontal or focal point directions, respectively, and orthogonal to η . Figure 6(b) illustrates the coordinate systems $\eta\zeta_E$, $\eta\zeta_H$, and $\eta\zeta_F$ where the incident point I represents the origin of the two-dimensional Cartesian coordinate systems. Equation (12) defines a parabolic strip in the plane passing through the elevation angle (θ) while Equations (13) and (14) define elliptical strips in the planes passing through horizontal or focal point (ϕ) planes. In each case, the strip's vertex is located on the point $I = (\eta = 0, \zeta_{E,H,F} = 0)$. The stack of these strips for each value of ϕ forms the double-curvature fitting surface. More information about the subject can be found in [1, 15].

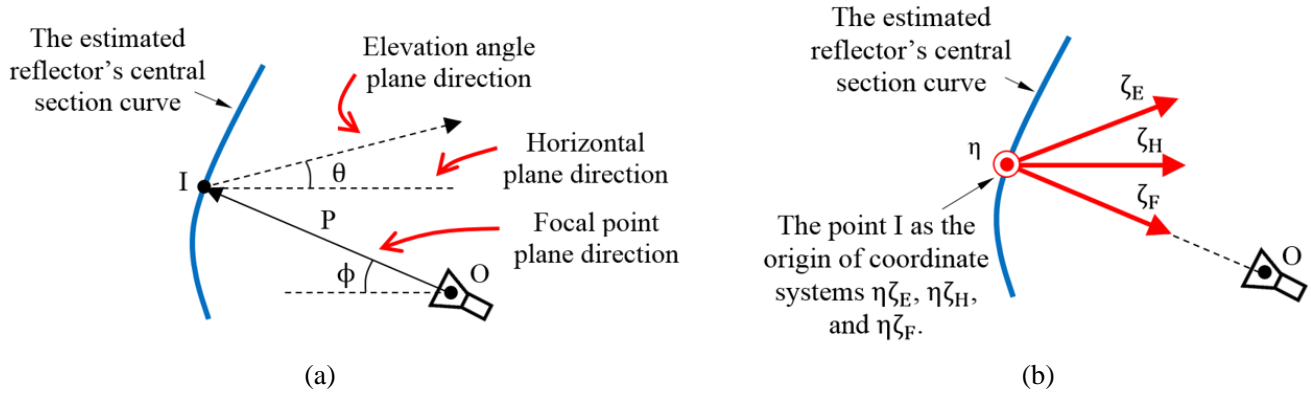


Figure 6. The estimated reflector's central section curve with its feeding horn in front of it. (a) The incident ray is shown with a solid arrow, and the reflected beam is shown with a dashed arrow. The horizontal direction is shown with a dashed line. (b) $\eta\zeta_E$, $\eta\zeta_H$, and $\eta\zeta_F$ are two-dimensional Cartesian coordinate systems for redesigning the reflector using elevation angle, horizontal, or focal point strips, respectively.

For evaluating the fitness of the fitted surface to the sampled points, two different kinds of errors are defined in the optimization algorithm with the names of E_{11} and E_{12} . Error E_{11} calculates the normalized sum of distances between each of the points sampled from the reflector surface and its corresponding point on the fitted surface. On the other hand, error E_{12} computes the normalized sum of absolute differences between the distance of any two points sampled from the reflector surface and the corresponding distance on the fitted surface. The resulting error for each optimization parameter vector is the sum of E_{11} and E_{12} , which is defined as E_1 and specifies the optimization algorithm cost function. Assuming that S_i is an arbitrary point sampled from the reflector surface where $i = 1, \dots, N$ and N is the number of the sampled points, S'_i is its corresponding point on the fitted surface, and $d(A, B)$ represents the distance between two arbitrary points A and B. Then the errors E_{11} , E_{12} , and E_1 for each of the optimization parameter vectors in the colony can be defined using Eqs. (15) to (17):

$$E_{11} = \frac{\sum_{i=1}^N d(S_i, S'_i)}{N} \quad (15)$$

$$E_{12} = \frac{\sum_{j=1}^N \left[\sum_{i=1}^N |d(S_i, S_j) - d(S'_i, S'_j)| \right]}{[N(N-1)]} \quad (16)$$

$$E_1 = E_{11} + E_{12} \quad (17)$$

By defining the optimization cost function as above and trying to minimize it through the optimization process, the undesired surfaces are less likely to emerge as the final optimization result effectively.

After evaluating the error for each of the optimization vectors (weeds) in the set (colony), they can be ranked according to their fitness. A specific portion of the set of weeds in the colony with the highest fitness values must be chosen as the plants to produce the next generation of seeds. The generated seeds will be distributed with normal distribution around their parent plants. The normal distribution's standard deviation (SD) will be reduced by each iteration in the optimization algorithm, from σ_{initial} for the first iteration to σ_{final} for the last one. The function σ that describes this reduction as a function of iteration number n , and nonlinear modulation index q , is described in Eq. (18):

$$\sigma(n) = \left(\frac{n_{\text{max}} - n}{n_{\text{max}}}\right)^q (\sigma_{\text{initial}} - \sigma_{\text{final}}) + \sigma_{\text{final}} \tag{18}$$

where n_{max} refers to the maximum number of iterations. The number of seeds each plant produces for the next generation has a direct relationship with its evaluated error, with the plants having a lower evaluated error producing a larger number of seeds for the next generation.

The above procedure repeats until the maximum number of generations are produced, and their errors are evaluated. Finally, the plant with the minimum value of estimated error is selected as the IWO optimization algorithm final solution, introducing the best-fitting surface to the sampled points. The flowchart of the proposed IWO process for finding the best-fitting surface to the sampled points using the three types of strips is presented in Figure 7. Also, more information about the IWO algorithm can be found in [17].

The flowchart of Figure 7 can be considered a subroutine in a more comprehensive process, as shown in Figure 8. Here, the same optimization quantities and also the sampled information are applied to the IWO algorithm in Figure 7 for finding the best-fitting surface to the sampled points using elevation angle (block 1.1, in Figure 8), horizontal (block 1.2 in Figure 8), or focal point (block 1.3 in Figure 8) strips. The estimated errors for these strip types are compared finally, and the strip type and optimization

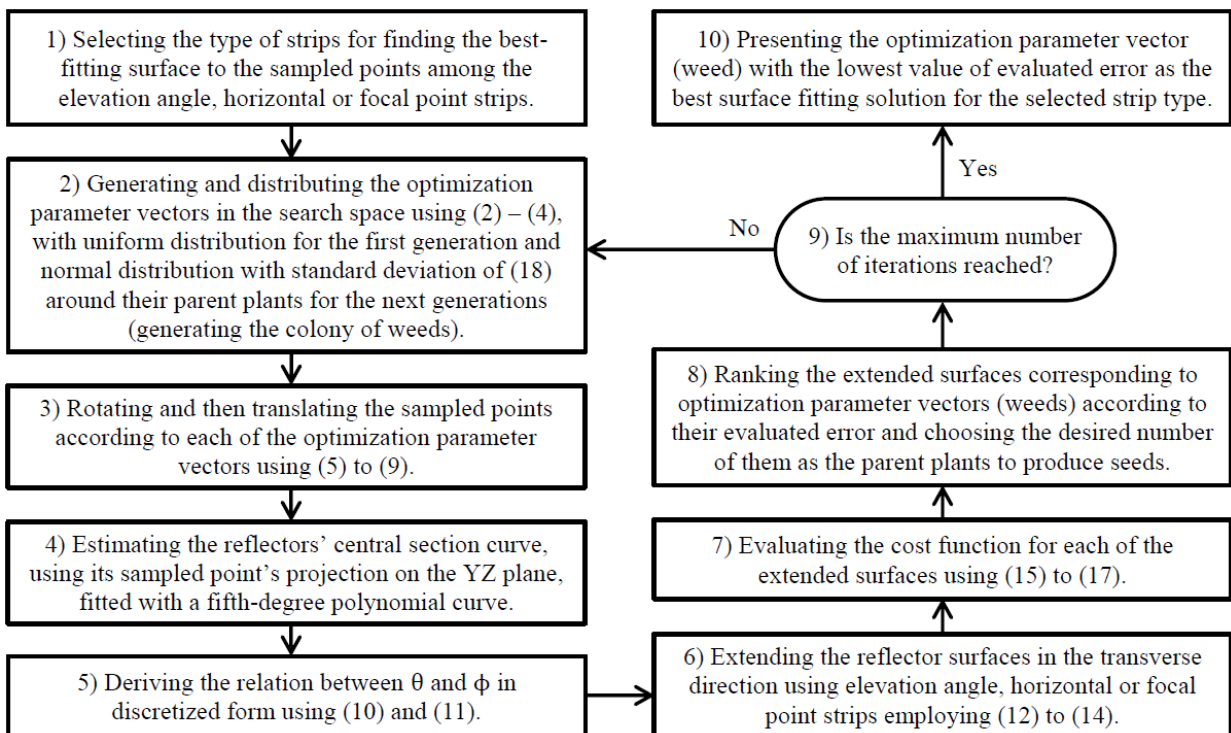


Figure 7. The proposed IWO flowchart for finding the best-fitting surface to the points sampled from the reflector using elevation angle, horizontal, or focal point strips.

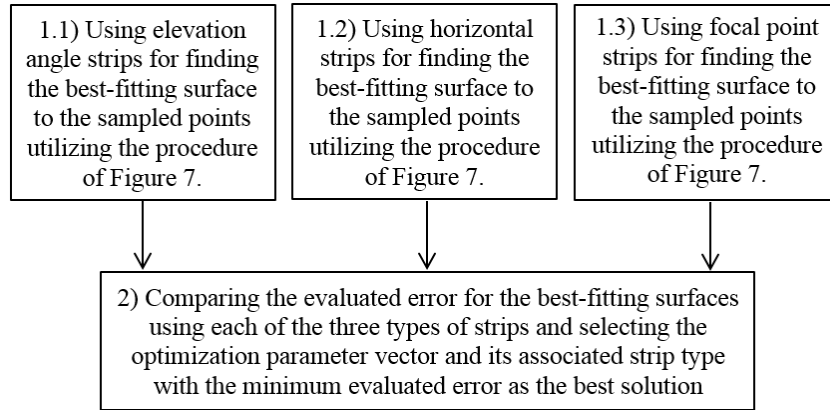


Figure 8. The recommended approach to discover the optimum strip type and the optimization parameter vector for finding the best-fitting surface to the sampled points using the IWO algorithm.

parameter vector which yields the minimum value of error will be chosen as the optimum solution for fitting a surface to the sampled points (block 2 in Figure 8) using IWO algorithm.

Currently, the optimization algorithm (Figure 7) is implemented in Matlab codes and is used to find the best-fitting surface to the sampled points using the three types of strips in three different execution runs. The employed optimization quantities are given in Table 2.

Figure 9 shows the evaluated normalized error (E_1) for the three types of strips as a function of the optimization iteration number. It can be seen that the resulting error at the end of optimization using horizontal strips is significantly smaller than the resulting error using elevation or focal point strips. Also, Table 3 gives the final normalized errors for the three types of strips after the optimizations. The

Table 2. The employed IWO algorithm quantities for finding the best-fitting surface to the sampled points using the suggested method.

| Optimization quantities | Value |
|---|--|
| Number of the initial population | 25 |
| Maximum number of iterations | 100 |
| Search space dimensions | 5 for redesigning using elevation angle or focal point strips and 6 for redesigning using horizontal strips |
| Maximum number of weeds population | 50 |
| Maximum number of generated seeds for each parent | 10 |
| Minimum number of generated seeds for each parent | 4 |
| Nonlinear modulation index (q) | 3 |
| Standard deviation initial values corresponding to the optimization parameter vectors V_E , V_H , and V_F | $\sigma_{\text{initial}}^E = \sigma_{\text{initial}}^F = (10, 10, 10, 30, 40)$ $\sigma_{\text{initial}}^H = (10, 10, 10, 10, 30, 40)$ |
| Standard deviation final values corresponding to the optimization parameter vectors V_E , V_H , and V_F | $\sigma_{\text{final}}^E = \sigma_{\text{final}}^F = (0.01, 0.01, 0.01, 0.01, 0.01)$ $\sigma_{\text{final}}^H = (0.01, 0.01, 0.01, 0.01, 0.01, 0.01)$ |

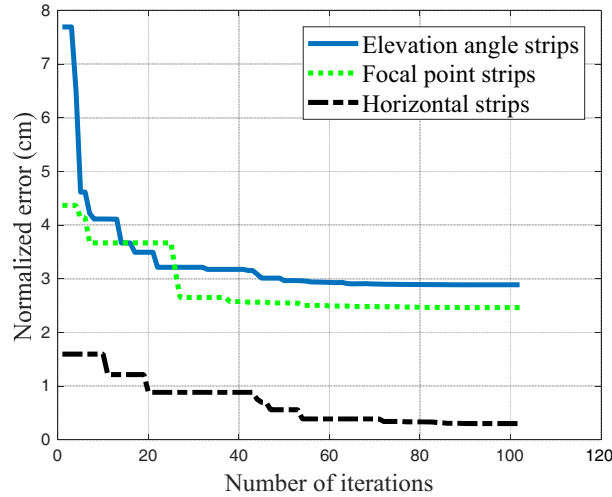


Figure 9. The normalized error (E_1) in the IWO algorithm versus the iteration number for fitting a surface to the sampled points, using elevation angle, horizontal, or focal point strips.

Table 3. Normalized errors (E_1) for each of the three mentioned methods at the end of the optimization algorithm.

| | Elevation angle strips | Focal point strips | Horizontal strips |
|------------|------------------------|--------------------|-------------------|
| E_1 (cm) | 2.89 | 2.46 | 0.30 |

Table 4. The final optimized parameters for the reflector redesigned using horizontal strips.

| Optimized parameters | Optimized values |
|----------------------|------------------|
| t_x (cm) | -0.4836 |
| t_y (cm) | 181.9730 |
| t_z (cm) | 110.3030 |
| α_x (deg) | 3.8300 |
| α_y (deg) | -0.0033 |
| α_z (deg) | 0.0597 |

evaluated error for fitting a surface to the sampled points using horizontal strips is about 0.3 cm, which is considerably small as compared to the reflector antenna’s dimensions and proves the geometrical similarity of the redesigned reflector with the reference one. Also, the optimized parameter values for redesigning the reflector using horizontal strips are given in Table 4.

2.3. Adjusting the Best-Fitting Surface’s Peripheral Contour

The best-fitting surface to the sampled points, obtained in the previous section, has an outer contour in agreement with the method used to obtain it; however, for some reason, the outer shape of the fabricated reflector may be different from the one initially designed. This difference may be due to the need to improve the antenna’s radiation pattern or its mechanical properties, such as reducing its weight or resistance to the wind. As stated in [15], a doubly-curved reflector designed using horizontal strips has a rectangular front view, different from the antenna illustrated in Figure 2(b). Hence, it is necessary to adjust the fitting surface’s outer contour according to the reference reflector, using the points sampled from its peripheral contour. This is done using Matlab codes, and Figure 10 illustrates the best-fitting surface before and after trimming its outer shape from different perspectives.

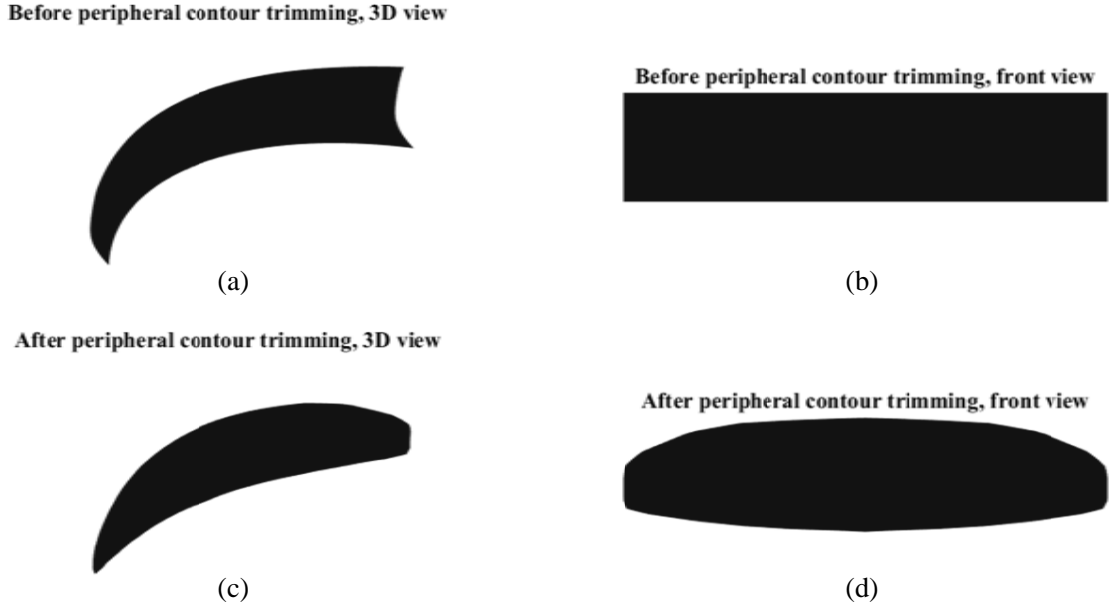


Figure 10. The best-fitting surface's silhouette in black color before (a), (b) and after (c), (d) trimming its peripheral contour from (a), (c) three dimensional and (b), (d) front perspectives.

2.4. Converting the Redesigned Reflector Surface to STL File Format

The fourth stage of redesigning the reflector is to convert the resulted surface, defined using a point cloud in a Matlab matrix, to a CAD file format applicable in the full-wave electromagnetic simulation software such as CST or HFSS. Among different choices, .stl is used as the destination file format. Its name is the acronym of Standard Triangle Language or Standard Tessellation Language and describes the object surface using a mesh of tiny triangles. The reason for this choice is that converting a Matlab matrix to this file format is relatively simple. Figure 11 shows the redesigned reflector in .stl file format.

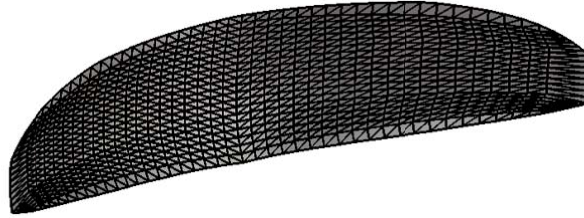


Figure 11. The redesigned reflector model in .stl file format, which is composed of a mesh of tiny triangles.

2.5. Further Modification of the Redesigned Surface by Considering Its Radiation Pattern Characteristics

In addition to the similarity between the redesigned and reference reflectors' geometry, it is necessary to consider the similarity between their radiation patterns as another criterion in the proposed redesign method. While the geometrical similarity between the redesigned and reference reflectors is evaluated using the cost function E_1 in Eq. (17), the sameness of their radiation pattern is assessed using the cost function E_2 as defined in Eq. (19).

$$E_2 = w_1 * (\Delta G)^2 + w_2 * (\Delta BW_{az})^2 + w_3 * (\Delta BW_{el})^2 + w_4 * (\Delta SLL_{az})^2 + w_5 * (\Delta \beta)^2 \quad (19)$$

Here, ΔG , ΔBW_{az} , ΔBW_{el} , ΔSLL_{az} , and $\Delta\beta$ are the differences between the redesigned and reference reflector antennas' gains, half-power beamwidths in the azimuth and elevation planes, average side-lobe levels in the azimuth plane, and parameter β , respectively. Especially, the parameter β is considered for the description of the cosecant-squared radiation pattern in the elevation plane and will be defined in the next section. Also, w_1 to w_5 are the weighting coefficients used to adjust the effect of the five parameters in the cost function E_2 .

If the value of E_2 or its variations are in an acceptable range defined by the designer, the redesigned surface will be selected as the optimum solution; otherwise, the optimization quantities or even the sampled information are modified to obtain a better-redesigned surface, and this process continues until an appropriately redesigned surface is achieved.

The optimization quantities modifications consist of increasing the IWO's initial population number, its number of iterations, its maximum number of weeds population, and its maximum and the minimum numbers of generated seeds for each parent plant, which are introduced in Table 2. Also, it is possible to estimate the reflector's central section curve with a curve other than fifth-degree polynomial as stated in Section 2.2.

Besides, if the IWO modifications do not satisfy the criteria for redesigning the reflector, the initial information can be sampled again with a larger amount and higher accuracy. Figure 12 illustrates the suggested approach in the form of a flowchart.

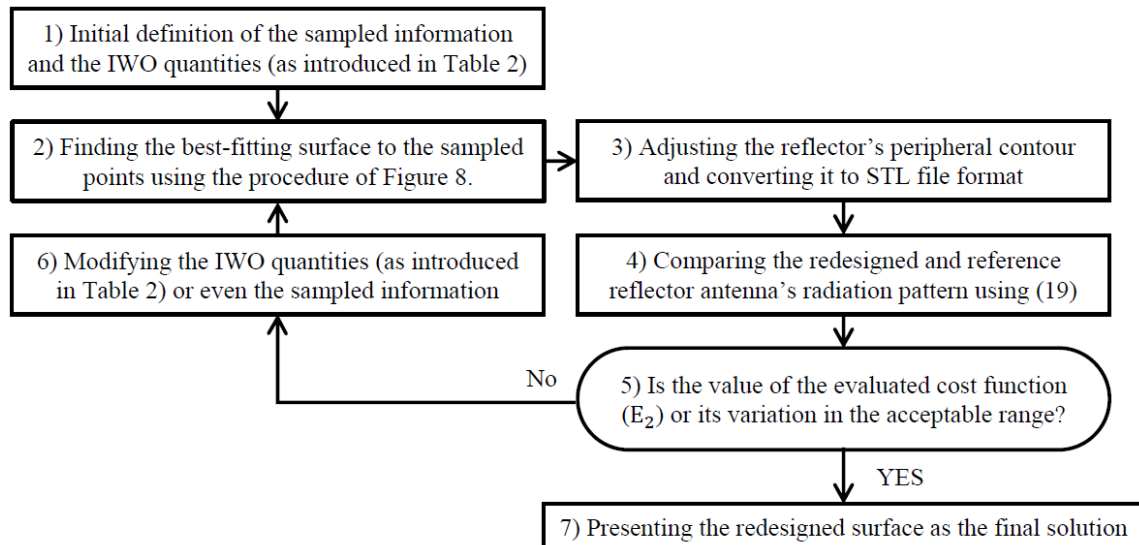


Figure 12. The flowchart of the suggested method for modifying the redesigned reflector according to its radiation pattern.

3. MEASURED AND SIMULATED RADIATION PATTERNS

By redesigning the UHF-band, double-curvature reflector antenna optimally, its radiation pattern is simulated and compared with the measured radiation pattern of the fabricated reflector and the simulated radiation pattern of the reflector's initial CAD model. The radiation pattern is simulated using CST simulation software, and the measurement is carried out using the outdoor measurement technique. Figure 13 shows the simulated and measured radiation patterns in the azimuth and elevation planes. As can be seen, there is good correspondence between the simulated and measured results in the elevation and azimuth planes.

For a better comparison of the results in the elevation plane, two parameters, α and β , are defined for a typical cosecant-squared radiation pattern, as shown in Figure 14. The parameter α defines the amount of gain difference between points A and B, where point A is defined in the boresight direction, and point B is in 9° offset from point A. The radiation power decreases in a cosecant-squared manner from point A toward point B. Besides, the parameter β defines the offset angle at the other side of the

boresight direction between points A and C, where the gain decreases sharply by an amount of 10 dB from point A toward point C.

Table 5 gives some quantitative information about the radiation patterns in Figure 13 regarding their gain (G), HPBW in the azimuth (BW_{az}) and elevation (BW_{el}) planes, average SLL in the azimuth plane (SLL_{az}), and the parameters α and β in the elevation plane. The results are substantially similar which emphasizes the efficiency of the proposed method in redesigning double-curvature reflector antennas.

However, some discrepancies between the measured and simulated results may be caused by the multipath effect during outdoor radiation pattern measurement or the deviation of the feeding horn antenna from its correct position and direction in front of the reflector. Besides, possible deviations of the fabricated reflector from its ideal, GO-based surface may cause some differences between the measured and simulated results. These differences may be due to imperfect initial fabrication or deformation of the reflector during its operation periods.

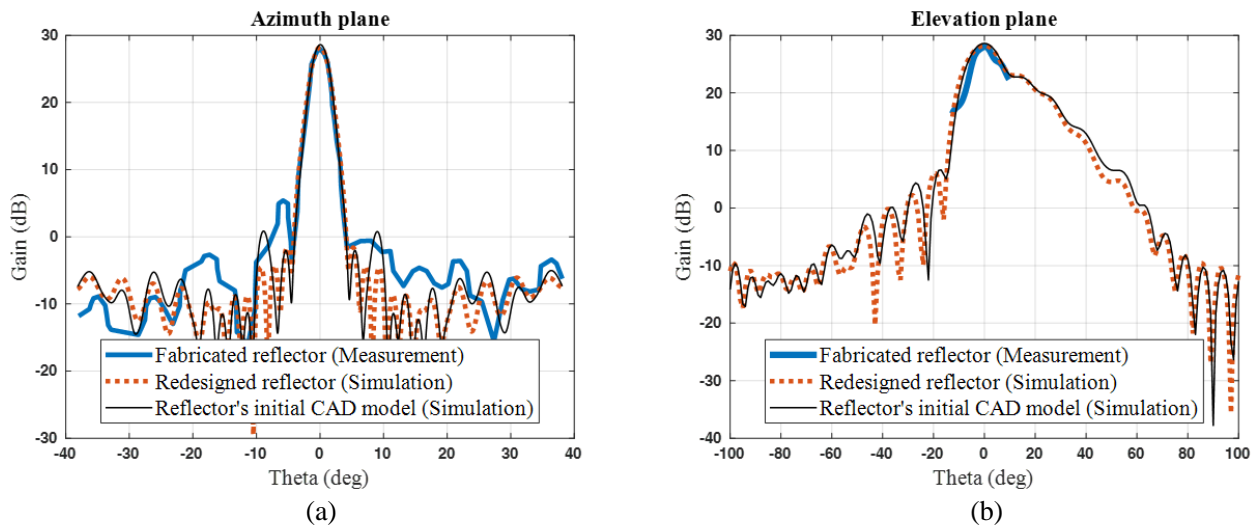


Figure 13. Measured radiation pattern of the fabricated reflector antenna (thick solid line) and simulated radiation pattern of the reflector antenna’s redesigned (dashed line) and initial CAD (thin solid line) model in the (a) azimuth and (b) elevation planes.

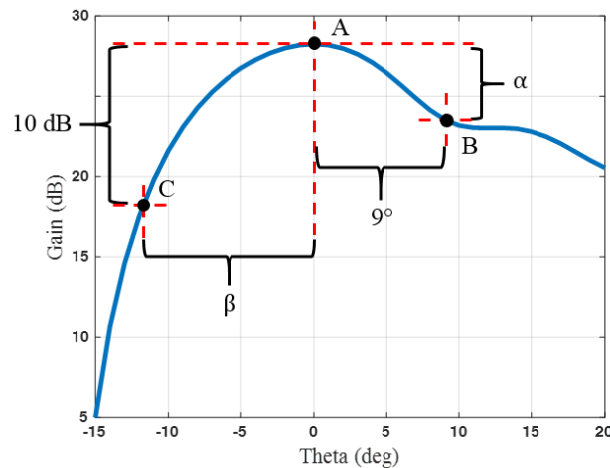


Figure 14. A typical cosecant-squared radiation pattern in the elevation plane with the parameters α and β defined on it.

Table 5. Some quantitative results of the measured radiation pattern of the fabricated reflector and the simulated radiation pattern of the redesigned and initial CAD model of the reflector in the azimuth and elevation planes.

| | Dimension | Measurement | Simulation | |
|---|-----------|----------------------|------------------------------------|----------------------|
| | | Fabricated reflector | Initial CAD model of the reflector | Redesigned reflector |
| Gain (G) | dB | 28 | 28.6 | 28.25 |
| HPBW in the azimuth plane (BW_{az}) | Degrees | 2.46 | 2.5 | 2.6 |
| HPBW in the elevation plane (BW_{el}) | Degrees | 11.49 | 12.7 | 13.5 |
| Average side lobe level (SLL_{az}) | dB | 25.76 | 30.64 | 29.85 |
| α | dB | 5.06 | 5.48 | 5.07 |
| β | Degrees | 9.66 | 10.51 | 11.7 |

4. CONCLUSIONS

Sometimes it is necessary to redesign a doubly-curved reflector antenna for reconstructing or repairing it according to a correct reference or examining its radiation pattern through full-wave simulations. One possible solution is to find the best-fitting surface to the points sampled from the reflector using available surface fitting approaches. Although these methods can yield a surface that is well-matched to the sampled points, their resulting surface is vulnerable to the imperfections in the reflector's geometry or imprecision in the sampled information, since they have no insight into the reflector's electromagnetic behavior. On the other hand, the suggested method uses geometrical-optics-based formulations for finding the best-fitting surface to the sampled points. In this method, the double-curvature surface is formed using elevation angle, horizontal, or focal point strips, and the surface fitting process is done in an IWO algorithm. As these formulations are generally used in the initial design of this kind of reflector, the resulting surface will be less vulnerable to the reflector surface defects or the sampled information inaccuracies, and the fitted surface will be most similar to the one initially designed using analytical approaches. Five or six optimization parameters are determined, depending on the type of strips used to surface fitting. Also, the sum of two kinds of normalized errors E_{11} and E_{12} are defined to find the best-fitting surface to the sampled points more reliably. Besides, the similarity between the redesigned and reference reflectors' radiation patterns is evaluated using a secondly-defined cost function in an iterative procedure which helps to find a more appropriate redesigned surface. The best-fitting surface to a UHF band, cosecant-squared radiation pattern reflector antenna is found using horizontal strips. The normalized error at the end of the optimization run is about 3 mm, which indicates the perfect geometrical similarity between the redesigned and fabricated reference reflector surfaces. Then the fitted surface's peripheral contour is trimmed to match the reference reflector's contour. Finally, the redesigned surface is converted to a CAD file with .stl format for further full-wave electromagnetic simulation using CST software. The simulated radiation pattern of the redesigned reflector is compared with the measured radiation pattern of the fabricated reflector and the simulated radiation pattern of the reflector's initial CAD model. Primarily, their results are investigated in terms of the antenna's gain, HPBW, and SLL in the azimuth plane and the parameters α and β in the elevation plane. Excellent correspondence is observed between the results in both planes. However, minor discrepancies between the results can be reduced by sampling more points from the fabricated reflector surface or using more robust quantities in the IWO algorithm. Besides, and some differences between the results may be due to imperfections in the reference reflector's surface, which are not present in the redesigned one, multipath effect, or deviation of the feeding horn antenna from its correct position and direction during the outdoor radiation pattern measurement. Therefore, it seems that the proposed method can be used to retrieve a double-curvature reflector antenna effectively.

REFERENCES

1. Dunbar, A. S., "Calculation of doubly curved reflectors for shaped beams," *Proceedings of the IRE*, Vol. 36, No. 10, 1289–1296, 1948.
2. Chu, L. J., "Microwave beam-shaping antennas," Army Signal Corps Contract No. W-36-039 sc-32037, 1947.
3. Silver, S., *Microwave Antenna Theory and Design*, Massachusetts Institute of Technology, Radiation Laboratory series, Boston Technical Publishers, 1964.
4. Balanis, C. A., *Antenna Theory Analysis and Design*, 2016.
5. Dastranj, A., H. Abiri, and A. Mallahzadeh, "Design of a broadband cosecant squared pattern reflector antenna using IWO algorithm," *IEEE Transactions on Antennas and Propagation*, Vol. 61, No. 7, 3895–3900, 2013.
6. Dastranj, A. A., H. Abiri, and A. R. Mallahzadeh, "Cosecant-squared pattern synthesis method for broadband-shaped reflector antennas," *IET Microwaves, Antennas & Propagation*, Vol. 8, No. 5, 328–336, 2014.
7. Foudazi, A. and A. R. Mallahzadeh, "Pattern synthesis for multi-feed reflector antennas using invasive weed optimisation," *IET Microwaves, Antennas & Propagation*, Vol. 6, No. 14, 1583–1589, 2012.
8. Mizusawa, M., S. Urasaki, S. Betsudan, and M. Limori, "A dual doubly curved reflector antenna having good circular polarization characteristics," *IEEE Transactions on Antennas and Propagation*, Vol. 26, No. 3, 455–458, 1978.
9. Winter, C., "Dual vertical beam properties of doubly curved reflectors," *IEEE Transactions on Antennas and Propagation*, Vol. 19, No. 2, 174–180, 1971.
10. Zornoza, J. A., R. Leberer, J. A. Encinar, and W. Menzel, "Folded multilayer microstrip reflectarray with shaped pattern," *IEEE Transactions on Antennas and Propagation*, Vol. 54, No. 2, 510–518, 2006.
11. Carrasco, E., M. Arrebola, J. A. Encinar, and M. Barba, "Demonstration of a shaped beam reflectarray using aperture-coupled delay lines for LMDS central station antenna," *IEEE Transactions on Antennas and Propagation*, Vol. 56, No. 10, 3103–3111, 2008.
12. Carluccio, G., A. Mazzinghi, and A. Freni, "Design and manufacture of cosecant-squared complementary reflectarrays for low-cost applications," *IEEE Transactions on Antennas and Propagation*, Vol. 65, No. 10, 5220–5227, 2017.
13. Arrebola, M., J. A. Encinar, and M. Barba, "Multifed printed reflectarray with three simultaneous shaped beams for LMDS central station antenna," *IEEE Transactions on Antennas and Propagation*, Vol. 56, No. 6, 1518–1527, 2008.
14. Holzman, E. L., "Pillbox antenna design for millimeter-wave base-station applications," *IEEE Antennas and Propagation Magazine*, Vol. 45, No. 1, 27–37, 2003.
15. Brunner, A., "Possibilities of dimensioning doubly curved reflectors for azimuth-search radar antennas," *IEEE Transactions on Antennas and Propagation*, Vol. 19, No. 1, 52–57, 1971.
16. Peter, L. and K. Šalkauskas, *Curve and Surface Fitting: An Introduction*, Computational Mathematics and Applications, Academic Press, 1986.
17. Mehrabian, A. R. and C. Lucas, "A novel numerical optimization algorithm inspired from weed colonization," *Ecological Informatics*, Vol. 1, No. 4, 355–366, Dec. 1, 2006.
18. Misaghi, M. and M. Yaghoobi, "Improved invasive weed optimization algorithm (IWO) based on chaos theory for optimal design of PID controller," *Journal of Computational Design and Engineering*, Vol. 6, No. 3, 284–295, Jul. 1, 2019.
19. Goldstein, H., C. P. Poole, and J. L. Safko, *Classical Mechanics*, Addison-Wesley series in physics, Addison Wesley, 2002.